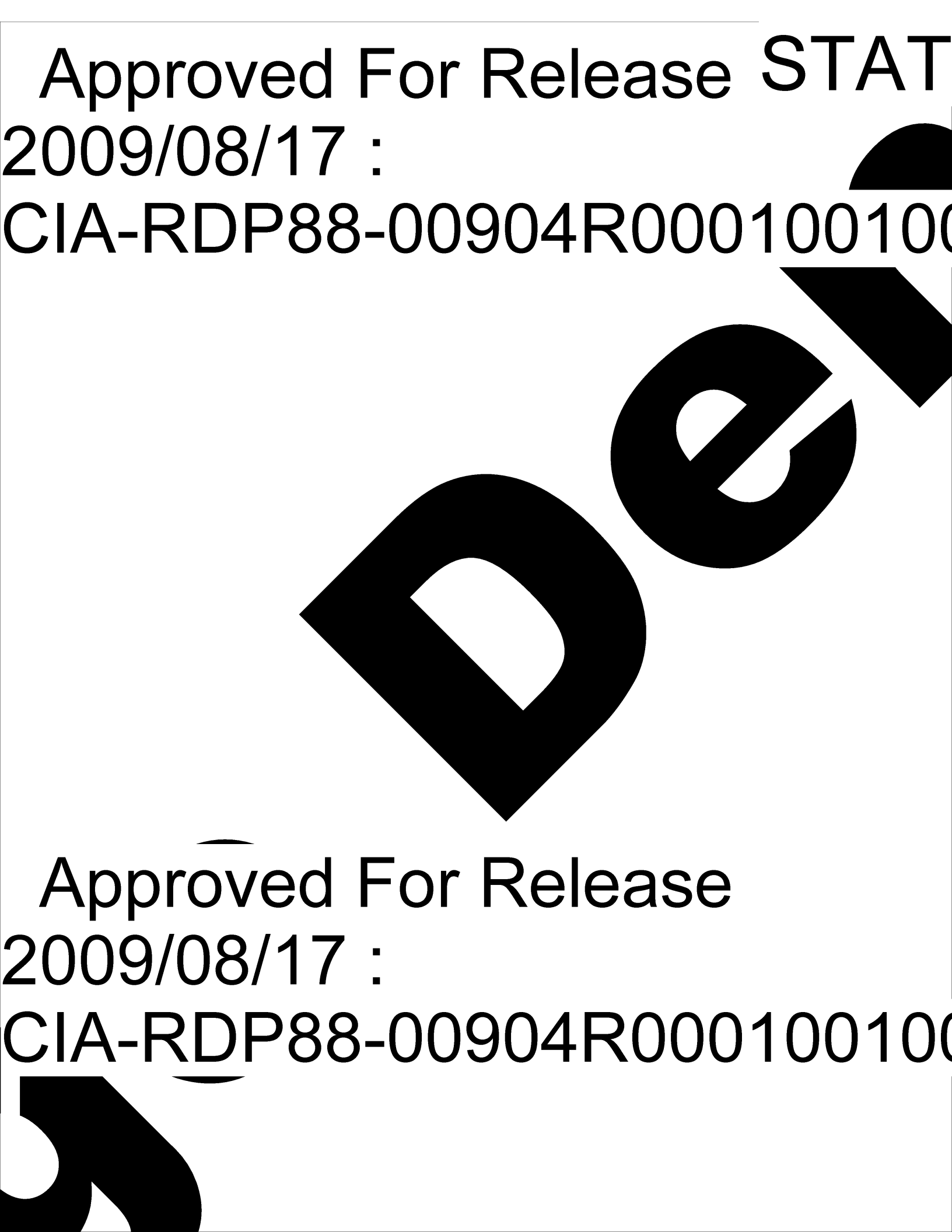

Third United Nations International Conference on the Peaceful Uses of Atomic Energy

A/CONF.28/P/328
USSR
May 1964
Original: RUSSIAN

Confidential until official release during Conference

HEAT REMOVAL FROM THE REACTOR FUEL ELEMENTS COOLED BY LIQUID METALS

V.I.Subbotin, P.A.Ushakov, P.L.Kirillov , M.K.Ibragimov, M.N.Ivanovsky, E.V.Nomophilov, D.M.Ovechkin, D.N.Sorokin, V.P.Sorokin

Lately liquid metals are more and more widely used in nuclear power engineering as coolants and working substances of cycles.

The paper contains the results of some liquid metals heat transfer investigations carried out at the Institute of Physics and Energetics.

I. HEAT TRANSFER TO LIQUID METALS FLOWING IN TUBES

The data available on heat transfer in tubes can be divided into two groups. The first group of the experimental data can be approximated by

$$Nu = 5 + 0.025\,Pe^{0.8}; \qquad (1)$$

the data of the second group fall much below this curve. This discrepancy is caused by the contact thermal resistance (R_k) between the wall and liquid metal. To exclude the influence of R_k upon the data treatment results, the data of the temperature distribution measurements were analysed for liquid metals in $T^+ - y^{++}$ coordinates and were presented by the following expressions [1]:

at $0 < y^{++} < 1$: $T^+ = y^{++}$; (2)

at $1 < y^{++} < 11.7$: $T^+ = 1.87 \ln (y^{++} + 1) + 0.065y^{++} - 0.36$; (3)

at $y^{++} > 11.7$: $T^+ = 2.5 \ln y^{++} - 1$. (4)

The dimensionless temperature distribution is independent in the given coordinate system of the Prandtl number Pr.

Equation (2) is obvious and no explanations are needed. Expression (4) describes the curve averaging the experimental data. Equation (3) is chosen to avoid the discontinuity in T^+ and $\frac{\partial T^+}{\partial y^{++}}$ at the edges of the layers (at $y^{++} = 1$ and $y^{++} = 11.7$).

Expression (4) is an approximate one and it cannot be utilized to calculate the eddy diffusivities. At the centre of the flow where the velocity is practically constant the temperature distribution is in fact nearly parabolical. However, this discrepancy does not greatly influence upon the calculation results of heat transfer coefficients, the latters may be found by the integra-

tion of the temperature distribution in the liquid metal flow. The integration yields formula (1). The equations similar to (1) have been individually established by N.I.Buleev and L.S.Kokorev in the USSR.

In practice, the heat transfer coefficients can diminish because of the contamination of the coolant and heat transfer surface. It was stated by means of the wall temperature measurements and those of the temperature distribution in fluid metals that the thermal resistance is mainly determined by the amount of oxides and other impurities concentrated near the wall. The magnitude of R_k depends on the tube diameter and the coolant velocity nearly in the same way as the laminar sublayer thickness. Thermal conductivity of the contaminated coolant layer near the wall proved to be proportional to the coolant thermal conductivity. The contact thermal resistance data for various liquid metals may be generalized with the help of dimensionless coordinates $\frac{R_k \lambda f}{d}$ – Re.

After the treatment of the temperature fields measured in the flows of various coolants over the wide range of Re and Pr, the eddy diffusitivities for heat were determined [2, 3]. Their values have a maximum at $0.2 < \frac{r}{r_o} < 0.3$ and approach zero when $\frac{r}{r_o} \to 1$. At the tube axis they are not equal to zero. Analysing the experimental data for mercury, water and air, it was found the eddy diffusitivities for heat are independent of Pr (Fig. 1). The following equations have been also obtained for a wide range of Re and Pr:

$$\frac{\epsilon_a}{\nu} = 2.04 \times 10^{-3} \text{ Re } [1 + (\frac{r}{r_o})^2 - 2 (\frac{r}{r_o})^3] - [0.329 + 8.36 \times 10^{-7} \text{ Re}] \times y^+ e^{-0.083 y^+} \quad (5)$$

$$\text{Nu} = 7.24 - \frac{9.5}{\lg \text{Re}} + 0.0153 \text{ Re}^{0.82} \text{Pr}^n \quad (6)$$

where $n = 0.58 - 0.18$ th $(0.8 \lg \text{Pr})$.

The relation between the eddy diffusitivities for heat and momentum $\epsilon = \frac{\epsilon_a}{\epsilon_\nu}$ was also determined. The magnitude of ϵ is a function of a radial distance; it also depends on the Reynolds number Re [3].

While measuring the turbulent temperature fluctuations in water and mercury flow, it was found, the temperature fluctuation amplitudes at the fixed point of floware in accordance with the normal distribution law.

The correlation coefficient R_r between the fluctuations at the points r_1 and r_2 diminishes from unity to zero when the distance $(r_2 - r_1)$ increases up to 8 – 12 mm (Fig. 2). The typical turbulence scale for radial direction L_r varies at $0 < \frac{r}{r_o} < 0.9$ relatively slightly and decreases rapidly in going from $\frac{r}{r_o} = 0.9$ to $\frac{r}{r_o} = 1$. The maximum value of L_r is equal to $0.1 r_o$ at $\frac{r}{r_o} = 0.7$. The turbulence scales for reciprocally perpendicular directions on a tube cross-section plane are nearly the same. The typical turbulence scales are considerably greater for axial direction than for radial one. For instance, $L_z = 4.7 r_o$ at $\frac{r}{r_o} = 0$. Thus, turbulent eddies are elongated towards the flow direction.

328

A correlation factor R_τ is a function of a time shift parameter τ and independent of zero time chosen (Fig. 2). Thus, the function describing the temperature fluctuations at a fixed point of turbulent flow is a steady normally distributed random function.

The density of the spectral function reaches the maximum value 0.6 at frequency ~ 0.8 c/s and is rapidly diminishing with the increase of perturbation frequency. Nearly all the heat (~98%) is transferred by turbulent perturbations with the frequency < 10 c/s (Fig. 3). The average lifetime is 0.1 sec. when $Re = 10^5$.

The heat transfer study for different liquid metals flowing in short tubes revealed that the starting section length where the temperature and velocity distributions are not fully established depends on the Reynolds number Re more strongly in case of liquid metals than in that of normal fluids [3].

2. TEMPERATURE FIELD IN A BUNDLE OF CIRCULAR FUEL ELEMENTS

The circumferential temperature distribution of the circular fuel elements depends on the bundle array geometry, fuel element properties, fluid properties and on its flow conditions

Analysis of the differential equations of fluid motion and of the heat transfer equations for the case of fuel elements in jackets leads to the following dependence for the region of fully-established temperature and velocity profiles.

$$T_f = \frac{t_w - \bar{t}_w}{\bar{q} R_2} \lambda_f = f\left(\frac{S}{d_2}\,;\ \phi;\ Pe;\ Pr;\ M_k\right) \tag{7}$$

The fuel element properties can be characterized by the criterion

$$M_k = \frac{\lambda_f}{\lambda_w} \cdot \frac{1 + \xi^{2k} m}{1 - \xi^{2k} m}\ , \tag{8}$$

where $m = \dfrac{\lambda_w - \lambda_o}{\lambda_w + \lambda_o}$, $(-1 \leqslant m \leqslant 1)$; K are the harmonic numbers of Fourier series by which function (7) is represented [4]. The equation similar to (7) can be also obtained for the Nusselt number Nu, averaged over the perimeter.

The fuel elements can be divided into the following groups according to their heat-conduction properties.

Group 1. The most general case. The criterion of the fuel elements similarity is expressed by formula (8). The other groups of fuel elements are the limiting values of this group.

Group 2. At the inner surface of the fuel element jackets (at $r = R_1$) the heat flux does not vary with angular position ($q \approx$ const) if $\lambda_w >> \lambda_o$

$$M_k \simeq \frac{\lambda_f}{\lambda_w} \frac{1 + \xi^{2k}}{1 - \xi^{2k}} \tag{9}$$

For thin-walled jackets ($\delta / R_2 << 1$):

$$M \simeq \frac{\lambda_f R_2}{\lambda_w \delta} \tag{10}$$

Group 3. At the inner surface of the fuel element jackets (at $r = R_1$) the temperature does not vary with angular position ($t \simeq$ const) if $\lambda_w \ll \lambda_o$

$$M_k \simeq \frac{\lambda_f}{\lambda_w} \frac{1 - \xi^{2k}}{1 + \xi^{2k}} \tag{11}$$

For thin-walled jackets:

$$M \simeq \frac{\lambda_f \delta}{\lambda_w R_2} \tag{12}$$

Group 4. The elements with jackets are equivalent to the fuel rods with the heat-conductivity λ_w if jacket thickness is great ($\xi^{2k} \ll 1$) or when the elements and jackets heat-conductivities are equal ($\lambda_o = \lambda_w$; $m = 0$). In these cases

$$M \simeq \frac{\lambda_f}{\lambda_w} \tag{13}$$

Group 5. Elements with jackets are equivalent to the fuel rods with heat-conductivity λ_o when the jackets are thin ($\delta/R_2 \ll 1$), and their influence may be neglected.

$$M \simeq \frac{\lambda_f}{\lambda_o} \tag{14}$$

The given classification of circular fuel elements can help choosing the thermal simulation. As simulators of the elements the tubes were used which were electrically heated to provide uniform heat fluxes at the inner surface. With the help of such tubes the fuel elements of the first and second groups with thin-walled jackets (10), (12) can be easily simulated as well as those of the 4th, 5th groups (13), (14). It is difficult to simulate the elements of 1, 2, 3 groups which have sufficiently thick-walled jackets, because the simulation conditions (8), (9),(11) at arbitrary K can be reduced to the following conditions for the model and "nature":

$$\frac{\lambda_f}{\lambda_w} \simeq \text{idem}, \qquad \frac{\lambda_w}{\lambda_o} \simeq \text{idem}, \qquad \xi \simeq \text{idem}.$$

But if one knows the harmonic, the contribution of which to the temperature distribution is the greatest, the use can be made of the approximate simulation. For example, for the case of triangular array the fundamental harmonic corresponds to $K = 6$. Similarity condition in that case is

$$\left(\frac{\lambda_f}{\lambda_w} \cdot \frac{1 + \xi^{12}}{1 - \xi^{12}} \right)_{\text{sim.}} \simeq \left(\frac{\lambda_f}{\lambda_w} \cdot \frac{1 + m\xi^{12}}{1 - m\xi^{12}} \right)_{\text{nat.}} \tag{15}$$

Temperature fields in fuel element simulators were studied, using bundles consisting of seven tubes (triangular array) or of nine tubes (square array). The tubes were electrically heated and surrounded by a test section shell with a special cross-section. Since the heat picked up by fluid is not uniform over the bundle cross-section due to non-heated shell effect,

the fluid temperature was measured at every duct exit. In calculations the fluid temperature in the ducts, associated with the central rod, was used. Such an investigation method has been experimentally tested with the bundle of 37 heated tubes. The data obtained for the bundles of 7 and 37 tubes were in a good agreement.

The temperature of the tube wall was measured with the sheath-type thermocouples, 0.5 mm O.D. They were inserted into the slots on the tube surfaces.

The bundles consisted of tubes,17.6 mm O.D., with $\delta = 2$ mm ($\xi^{12} = 0.045$). The tubes were thick-walled enough to assume the tubes in the triangular array to be equivalent to the rods of the same thermal conductivity ($\xi^{12} = 1$). This assumption is less correct in case of square array (the number of the fundamental harmonic k = 4; $\xi^{8} = 0.127$.

The close bundles of stainless steel cooled by mercury (Pr=0.022 – 0.025) and water (Pr=2.4 – 4.8) were studied ($\frac{\lambda_w}{\lambda_f} = 1.85$ and 24, respectively) [4]. In runs with NaK (78% K, Pr = 0.022 – 0.024) the close bundles of stainless steel ($\frac{\lambda_w}{\lambda_f} = 0.69$) and copper ($\frac{\lambda_w}{\lambda_f} = 16.3$) were used. The test section shell was heated only in the runs with the copper bundle which had high thermal conductivity.

In these runs the contact thermal resistance did not take a noticeable part, since liquid metals were continuously purified from oxides. For instance, the amount of hydrogen in NaK did not exceed 10^{-3} weight percentage, and there were no insoluble oxides. The heat transfer data for mercury and NaK flowing in circular tubes, obtained under the same conditions, are in a good agreement and described by (1).

The circumferential temperature and heat flux distributions in the rods (or in the thick-walled tubes) in close bundles are shown in Fig.4. The heat flux distribution in a rod was found analytically

$$\frac{q}{\bar{q}} \simeq 1 - \sum_k k \frac{A_k}{M_k} \qquad (16)$$

$$\text{at } T_f = \sum_k A_k \cos k\phi \qquad (17)$$

The results obtained for the copper bundle are not plotted in Fig.4, as the temperature non-uniformity was insufficient in this case ($T_f^{max} < 0.02$). The data for fluid metals, given in Fig. 4, are averaged over the range $80 < Pe < 550$. In this range the temperature non-uniformity decreases about 1.3 – 1.5 times with Pe increase, and for mercury – about 1.1 – 1.15 times, respectively for square and triangular arrays. The data for water are averaged over the range $10^4 < Re < 2.10^4$ where the influence of Re on the temperature profile is insufficient.

The values of Pr and $\frac{\lambda_w}{\lambda_f}$ for water greatly differ from those for liquid metals, however, the temperature and heat flux non-uniformity differ not so greatly; it is interesting that in case of water cooling the temperature non-uniformity is the least. The temperature non-uniformity for a square array is greater than for triangular one.

The following is stated on the basis of data considered, analytical calculations and other experimental results. The dimensionless temperature non-uniformity for fuel rods without jackets is nearly proportional to $\frac{\lambda_w}{\lambda_f}$. As for thick-walled tubes, the value V slightly depends on ξ (on tube thickness).

In case of thin-walled tubes T_f depends rather slightly on $\frac{\lambda_w}{\lambda_f}$. Hence, T_f also slightly depends on the tube wall thickness since the relative thermal conductivity variation is equivalent to that of tube wall thickness (see formulas 10 and 12).

While increasing a pitch: diameter ratio, the value of the similarity criterion M_k is diminishing. Thus, even for $S/d_2 = 1.1$ the circumferential temperature non-uniformity is about 5 times less than for close packing, i.e. it becomes insufficient. Therefore, when $S/d_2 > 1.1$, the criterion M_k may be excluded from equation (7) and in most cases the circumferential temperature non-uniformity may be neglected.

The experimental data obtained for close packings with a triangular array are approximated by the formula:

$$Nu = 0.15 \left(\frac{\lambda_w}{\lambda_f}\right)^{0.02} Pe^{0.3 + 0.04 \sqrt{\frac{\lambda_w}{\lambda_f}}} \qquad (18)$$

$$Pr \ll 1;\ 80 < Pe < 600;\ 0.69 < \frac{\lambda_w}{\lambda_f} < 16.3$$

The data for square arrays are given in [4].

From the experiments with bundles ($S/d_2 = 1.1 - 1.5$) it is found that the heat transfer coefficients do not practically depend on the pitch in the given S/d_2 range if the rod diameters and mercury velocities are the same.* The experimental data on heat transfer to liquid metals for bundles with a triangular array are described by the formula

$$Nu = 0.58 \left(\frac{d_r}{d_2}\right)^{0.55} Pe^{0.45} \qquad (19)$$

$$80 < Pe < 4000;\ 1.1 < \frac{S}{d_2} < 1.5.$$

The heat transfer coefficients in formulas (18, 19) are defined by $\bar{\alpha} = \frac{\bar{q}}{t_w - t_f}$, where t_f is the fluid temperature in the ducts associated with the central rod. As a characteristic dimension an equivalent diameter of a duct is taken:

$$d_r = d_2 \left[\frac{2\sqrt{3}}{\pi} \left(\frac{S}{d_2}\right)^2 - 1\right]$$

The experimental data on heat transfer to liquid metal flowing in-line through a bundle of circular rods are presented in Fig. 5 where the following symbols are taken:

---

* The experiments were carried out with the partaking of Zhukov A.V., Krivtsov V.A. and Orlov Y.I.

$$\psi = \frac{Nu}{\left(\frac{\lambda_w}{\lambda_t}\right)^{0.02} Pe^{0.3} + 0.04} \qquad \text{for close packing and}$$

$$\psi = \frac{Nu}{\left(d_r/d_2\right)^{0.55} Pe^{0.45}} \qquad \text{for the bundles with } \frac{S}{d_2} > 1.$$

The heat transfer peculiarities in bundle are also observed in case of water cooling. The fully-established values of the Nusselt numbers Nu averaged over the perimeter for water flowing in-line through close-packed rod bundles with triangular and square arrays are described by the formula

$$Nu \simeq 0.01\, Re^{0.8} Pr^{0.43}; \qquad 400 < Re < 50{,}000 \qquad (20)$$

As a characteristic dimension an equivalent diameter of a duct is taken. Point scattering relative to the averaging curve does not exceed ±15 per cent.

At present some actual material is available on heat transfer to water and air flowing in-line through a bundle of rods with $\frac{S}{d_2} > 1$. The most data for water agree with the formula suggested by Weisman [5]:

$$Nu \simeq C\, Re^{0.8} Pr^{1/3}, \qquad (21)$$

where for the triangular array with $1.1 < \frac{S}{d_2} < 1.5$ $C = 0.026 S/d_2 - 0.006$,

and for the square one with $1.1 < \frac{S}{d_2} < 1.3$ $C = 0.042\, S/d_2 - 0.024$.

At $\frac{S}{d_2} \simeq 1.15$ formula (21) coincides with the formula for a circular tube. The experimental data for water are given in Fig. 6.

The data on heat transfer to air are more discrepant. Some of them agree well with the formula for a circular tube and the other ones agree neither with the formula for a circular tube nor with formula (21). It is seen, for instance from [6]. Thus, there is no reason to regard the problem of heat transfer to normal coolant flowing through a bundle of rods as finally solved one.

The data available for liquid metals and normal fluids show that the use of the formulas, obtained from the experiments with circular tubes, for calculating the temperature field of rod bundles (using the equivalent diameter) can lead to serious errors in many cases.

The influence of various parameters on the temperature field of fuel elements, arranged in a bundle, can be determined by approximate calculations. For instance, the predicted data for a slug flow give a good idea about a circumferential temperature and heat flux distribution in rods and thick-walled tubes. There is also a good coincidence between the calculations for a slug flow and the temperature field measurements for NaK flowing in a close-packed bundle of thick-walled tubes ($\xi = 0.93$).

In calculations of the slug flow neither the "stagnant" zones near the line of the tubes contact are taken into account, nor the turbulence. The influence of these factors is apparently

insufficient or they compensate one another. Therefore, the tube temperature non-uniformities predicted fall close to the measured ones.

3. THE MEAN COEFFICIENTS OF HEAT TRANSFER IN SHELL-AND-TUBE EXCHANGERS

The investigation was carried out with the partaking of Suvorov M.Y. and Kolotvin A.M.

The mean values of the shell side heat transfer coefficients were obtained for Na-K alloy. Sodium at a higher temperature than NaK temperature was flowing through the tubes of heat exchangers. Every heat exchanger consisted of seven tubes and a shell of a special cross-section shape.

During the experiments the mean coefficients of heat transfer from sodium to sodium-potassium alloy were measured. From these coefficients and the heat transfer coefficients to sodium, calculated according to (1), the mean values of the shell side heat transfer coefficients were determined.

$$\text{At } 1.1 < \frac{S}{d_2} < 1.4;\ 60 < {}^{l}/_{d_2} < 260;\quad 200 < Pe < 1200$$

the experimental data are approximated by (Fig. 7):

$$Nu = 8\left[\frac{d_r}{l} + 0.027\left(\frac{S}{d_2} - 1.1\right)^{0.46}\right] Pe^{0.6} \qquad (22)$$

As a characteristic dimension an equivalent diameter was taken. In Fig.7

$$\psi = \frac{Nu}{{}^{d_r}/_{l} + 0.027\,({}^{S}/_{d_2} - 1.1)^{0.46}}$$

The mean values of the shell side Nusselt numbers Nu also depend on ${}^{S}/_{d_2}$, as in the case of fuel rod bundles. It is noticeable that the relationship Nu versus Pe for heat exchangers is more strong ($Pe^{0.6}$) than for fuel rod bundles ($Pe^{0.4}$), and the heat transfer stabilization occurs at higher values of ${}^{l}/_{d_r}$. It is well in agreement with the data of [8].

The values of the Nusselt numbers Nu for heat exchangers (19) differ greatly from those (22) for bundles with heat generation. The reasons for the difference are the following. The mean values of the shell side heat transfer coefficients are influenced by a starting section and obtained for the case of the heat flux, distributed non-uniformly over the length. These reasons, are not the main ones, since for the great values of ${}^{l}/_{d_r}$ the influence of the starting section is negligible, and the influence of the heat flux non-uniformity is comparatively small.

The main reason for the difference is a great influence of a non-heated shell upon the fluid temperature field. While determining the heat transfer coefficients from Na to NaK, the mean cup-mixing temperature is used; the latter differs greatly from the local ones. Since the fluid temperature is not uniform over the heat exchanger cross-section, the different tube rows have different heat transfer intensities. The effect indicated diminishes very slowly with the increase of the tube number. It may be neglected only when the number of tubes is very great, as an approximate calculation has shown.

The difference of the data for heat exchangers and bundles can be estimated from the consideration of the following simplest problem. Assuming that the fluid temperature in the heat exchanger tubes is nearly constant (the assumption corresponds to the experimental conditions), the heat transfer coefficients are constant over the tube length, and there is no heat exchange between the ducts of the bundle,* the following formula can be derived:

$$\frac{Nu}{Nu_2} \simeq \frac{-8 \ln Nu_1}{d_r N Pe \ln [(1-\mu) \exp(-A_I) + \mu \exp(-A_{II})} - R_{\alpha_1} \qquad (23)$$

where Nu_1 is the Nusselt number for the central zone of the fuel rod bundle; Nu_2 is the mean value of the shell side Nusselt number; n, N are the number of tubes and ducts in the heat exchanger, respectively; μ is the portion of the peripheral ducts (i.e. the ducts associated with the shell); R is the thermal resistance between the hot liquid and the outer tube surface.

$$\alpha_1 \equiv \frac{Nu_1 \lambda_f}{d_r}; \qquad A \equiv \frac{kPl}{C_p \gamma v}; \qquad k, P, v \quad \text{are}$$

1) the heat transfer coefficient between Na and NaK,
2) the heat transfer circumference, 3) the volume flow rate for central (Index I) and peripheral (Index II) heat exchanger zones; when $n \to \infty$; $Nu_1/Nu_2 \to 1$.

The approximate calculations with the help of (23) yield the results, which qualitatively agree with the experimental data. It was found that the difference between Nu_1 and Nu_2 decreases with the increase of the Peclet number Pe and $Nu_1 > Nu_2$. Thus, the relationship $Nu_1 = f(Pe)$ must be slighter than $Nu_2 = f(Pe)$ and it is seen from the experiments. While treating the experimental data for bundles with $S/d_2 > 1$ and taking as the determining temperature drop ("wall-liquid") the difference between the averaged over the length rod temperature and the mean mercury temperature for the whole bundle the Nusselt numbers Nu_1 proved to be proportional to $Pe^{0.65}$.

A fairly great length of a stabilization section of the mean Nusselt numbers Nu for heat exchangers can be explained by the fact that the heat exchange between the neighbouring ducts is relatively small.

The experimental and predicted results, mentioned above, show that the data obtained from the experiments with heat exchangers may not be used directly for the calculations of fuel element bundles.

4. PECULIARITIES OF HYDRODYNAMICS IN ROD BUNDLES

When a duct has sufficiently smooth walls and there are no "stagnant" zones, the pressure drop law under turbulent flow conditions coincides usually with that for circular tubes if the equivalent diameter is taken as a characteristic dimension. There is no such coincidence for ducts of a more complicated shape.

*The experiments show that the heat exchange between the ducts of the bundle is negligible over the wide range of Pe and l/d_r.

326

The calculations and the experiments show that for close-packed bundles near the line of rods contact there are "stagnant zones" (i.e. the zones where the velocity is small). In this case the shear stress varies with the angular position. Friction factors for close-packed bundles with triangular and square arrays (in processing the equivalent diameter was used) are nearly the same and equal to 60 – 65 per cent of those for circular tubes [4, 9, 10].

Sometimes good results can be obtained with the help of the method [11] to calculate approximately friction factors for ducts of a complicated cross-section shape. The method consists in the substitution of the duct cross-section by such a cross-section when the following condition is satisfied:

$$\frac{\zeta}{\zeta_0} = \left(\frac{P'}{P}\right)^{1.25} \left(\frac{\omega'}{\omega}\right)^{-3} = \min, \qquad (24)$$

where ζ, ζ_0 are the friction coefficients for the duct and the circular tube, respectively. P', ω' are the wetted perimeter and the cross-section area of the duct obtained after the substitution. The calculation of the ducts in close-packed rod bundles, carried out by Papovyants A.K. and Ushakov P.A., yielded the following values of the friction factors:

Array type	Predicted values	Experimental values
Triangular square	$0.68\zeta_0$	$0.63\,\zeta_0$
	$0.685\zeta_0$	$0.63\zeta_0$

The available data on pressure drops in bundles with $\frac{S}{d_2} > 1$ are rather discrepant. In general, there is a tendency of increasing the friction factors with the growth of the pitch: diameter ratio $\frac{s}{d_2}$. It is probably caused by the effect of the secondary fluid currents in the bundle ducts. It is also possible that the experimental results involve the peculiarities of the bundles under investigation (e.g. the influence of rod bowing, the shape of the shell, etc.).

At present the most reliable method of determining the pressure losses in the reactor channels is a direct experimental measurement of the pressure drops in the channels or their models.

5. HEAT TRANSFER IN BOILING OF LIQUID METALS AND IN CONDENSATION OF THEIR VAPOURS

The investigation of heat transfer in the boiling of liquid metals was carried out with the participation of A.A. Ivashkevitch and A.P.Kudryavtsev. Liquid sodium was boiling on a horizontal surface under free convection conditions. It was at its own vapour pressure in the stainless steel tank, 160 mm in diameter and 280 mm high. The height of sodium layer was 150 — 200 mm. From the outside the tank was surrounded with the compensation heaters.

The heat transfer horizontal surface,38 mm in diameter, was placed at the same level as the tank bottom. Heating was realized by electron bombardment of the heat-conducting wall. The electrons emitted from a spiral tungsten cathode were accelerated by the anode voltage controlled in the limits 0 – 10 kv.

The sodium vapour was condensed in an air-cooled condenser placed at the upper part of the tank. The sodium vapour pressure was measured by the transmitter of a compensation type with an inductive "null instrument" (the sensitivity is ~ 1 mm Hg).

In some experiments the heat transfer coefficients were measured on the heat-conducting wall consisting of three layers. The stainless cylindrical cup was cast in vacuum with copper. After some mechanical treatment the copper surface was plated with about 20 μ of nickel to protect copper from sodium attack. In some experiments the plating was washed away and sodium got into contact with copper. In other cases the heat-conducting wall consisted of two layers (stainless steel,copper); sodium boiled on the stainless steel surface.

The wall temperature was measured by two chromel-alumel thermocouples (0.2 mm) covered with corundum insulation. They were installed in copper by means of casting. Such an installation gave high measurement accuracy of the heat transfer surface temperature (inertia was slight). The temperature distribution in sodium and vapour versus distance from bottom was measured with a movable thermocouple, its position could be determined with the accuracy ±0.2 mm. Sodium temperature was also measured with fixed thermocouples.

To investigate the burnout thermal fluxes the heat-conducting wall was made of nickel-base high temperature alloy or of molybdenum. The burnout onset was seen from a sharp increase of the wall temperature after a slight (1 – 2%) increase of the thermal flux.

To purify sodium periodically with a cold-trap and take sodium samples by the vacuum distillation method, the closed circulation loop has been provided.

The measurement method of the boiling coefficients and the burnout thermal fluxes was preliminarily tested in water boiling at atmospheric pressure.

It was found that sodium on stainless steel and nickel surfaces could be considerably overheated relative to the saturation temperature t_s (up to 100° and above). The whole volume of sodium was also considerably overheated. In this case there was no boiling on the heat transfer surface even when the thermal fluxes were great (~$10^6 \frac{kcal}{m^2 h}$). From the wall the heat was being removed by conduction and convection, and the evaporation from sodium surface took place. The measurements with the movable thermocouple showed that the temperature difference between sodium and vapour was great enough. Such temperature conditions lasted sometimes dozens of hours.

It was stated experimentally that there were two boiling conditions for sodium, i.e. stable and unstable ones. Under stable boiling conditions rather small fluctuations of the wall temperature were observed while great fluctuations (up to 100° and above) were characteristic of unstable boiling conditions. The frequency of temperature fluctuations under stable boiling conditions is higher than under unstable ones. On nickel and stainless steel surfaces there were observed both boiling conditions. On copper surfaces the boiling conditions were always stable. Both conditions could exist for a long time. Temperature drop on the sodium surface sharply decreased when passing from natural convection to unstable boiling and became insufficient in nucleate boiling.

The measurements with the movable thermocouple showed that practically there was no temperature gradient in boiling sodium, excluding the layer of several-mm thickness near the

wall. The temperature fluctuations of this layer were similar to the wall temperature fluctuations.

Typical variations of the heat-conducting wall temperature with time are presented in Fig. 8. The record was made with a potentiometer of EPP-09 type when sodium temperatures were fixed and thermal fluxes were constant. The diagram sections a, b, c correspond to the heat transfer without boiling. At the final points of these sections sodium temperature and the "wall-liquid" temperature drive suddenly decrease due to sodium boiling up. The transition is accompanied by loud strokes and the pressure rise in the tank. The sections d, e, f correspond to the unstable sodium boiling and the sections g, h do to the stable one.

The boiling coefficients obtained experimentally are presented in Fig. 9 ($\alpha \frac{kcal}{m^2 h\,^oC}$; $q \frac{kcal}{m^2 h}$). Here the available data on heat transfer are also presented when sodium is boiling on outer tube surfaces [12, 13] and NaK – on a plane surface [14].

The experimental data in Fig. 9 can be qualitatively divided into three groups. The first group corresponds to the case when the heat is removed by convection and heat conductivity, and no boiling occurs. The experimental data of this group are approximated by the curve according to $\alpha = 100 q^{1/3} \frac{kcal}{m^2 h\,^oC}$. The formula describes the data obtained with the same apparatus when no boiling occured ($t_w << t_s$).

The second group of the experimental data corresponds to the nucleate boiling. The curve averaging the data is approximated by the formula

$$\alpha \approx 4 q^{2/3} \frac{kcal}{m^2 h\,^oC} \qquad (25)$$

There exists a definite relation between the fluctuation amplitude and the division of the experimental data on nucleate boiling heat transfer (See Fig.9), namely, the higher boiling coefficients correspond to the lower temperature fluctuations (Cf. Figs 8 and 9).

The experimental data of the third group fall between the first group and the second group. The lower the amplitude and the higher the temperature fluctuation frequency are, the nearer the data of this group are to the nucleate boiling data.

In the investigated range of parameter variation the dependence $\alpha = f(p_s)$ proved to be slight. The values of burnout heat fluxes in sodium boiling under free convection conditions (Fig. 10) are presented by the formula:

$$q_{kp} = (1.5 + 1.3 p_s) 10^6 \frac{kcal}{m^2 h\,^oC} \qquad (26)$$

$$0.015 < p_s < 1.2 \text{ atm}$$

The data of [13] are in agreement with formula (26).

It is interesting to note that the burnout occurs earlier for the case of unstable boiling. For example, when $p_s \approx 0.35$ atm the values of q_{kp} for nucleate and unstable boiling differed by 70 per cent (the points a, b are given in Fig.10). Sodium boiling was studied visually with the aid of x-rays, the image was projected on the image converter screen. The sizes of vapour bubbles were seen to be greater for sodium boiling than for water boiling at the atmospheric pressure under the same conditions.

328

The condensation of "immovable" potassium vapour on a plane stainless steel surface has been studied. A foil sheet, 110x60 mm, 0.2 mm thick, served as the condensation surface, the former was brazed with a silver solder to a massive copper parallelepiped. The thermocouples, 0.8 mm O.D., were inserted in copper. The condensation was photographed through special glass windows.

After 20 minutes of operation at 450°C the wall got completely wetted and the condensation became filmwise. The potassium vapours were pale blue-green by daylight.

The heat transfer coefficients at 400 – 700°C, pressures 0.006 – 0.56 atm and heat fluxes $60.10^3 - 280.10^3 \frac{kcal}{m^2 h}$ were $15.10^3 - 25.10^3 \frac{kcal}{m^2 h\,°C}$, i.e. they were much less than the ones calculated with the account of condensate film thermal resistance only. The decrease of the heat transfer coefficients may be caused by the thermal resistance at the solid-liquid interface and by the thermal resistance at the vapour-liquid interface associated with the phase transition or with some amount of non-condensables available.

To investigate the influence of the factors indicated, the measurements have been carried out of the temperature distribution in potassium vapour, condensate and in the heat-conducting wall. For this purpose a movable thermocouple in a stainless sheath, 0.5 mm O.D., was used. The condenser was made as a cylinder of stainless steel. The cylinder was cooled from below by water. At the top of the cylinder there was a 8-mm deepening filled with condensate. The wall temperature field was measured by inserting a movable thermocouple into a narrow (0.95 mm) vertical slot cut in the wall.

The measurement at 320 – 640°C, 8.10^{-4} – 0.28 atm and $(8 - 18).10^4 \frac{kcal}{m^2 h}$ revealed that there was no contact thermal resistance between the stainless steel wall and condensate.

At low pressure the "temperature jump" was found at the vapour-liquid interface; it decreased with the pressure increase (Fig. 11). The value of the "temperature jump" agrees well with the predictions of the kinetic theory of gases; the condensation coefficient is assumed to be equal to unity and correction is made for convective vapour velocity towards the condensation surface [15], (Fig. 12).

As preliminary experiments show, the values of the condensation heat-transfer coefficients for the case of potassium vapour, flowing in a horizontal circular tube, are nearly the same as for the condensation on a plane surface. The radial component of the potassium vapour velocity has an influence upon the pressure drop for the condensation tube.

328

NOMENCLATURE

The following nomenclature is used:

r_o = radius of tube ($d = 2r_o$; $y = r_o - r$);

l = heated length;

P, p = heated perimeter; wetted perimeter of duct;

ω = cross-section area of the duct;

$d_r = \frac{4\omega}{p}$ = equivalent diameter;

R_1, R_2 = inner radius, outer radius of the tube (of the fuel element jacket);

$$(d_1 = 2R_1;\ d_2 = 2R_2;\ \xi = \frac{R_1}{R_2});$$

δ = wall thickness;

S = pitch, distance between tube (rod) centres;

λ_f, λ_w, λ_o = thermal conductivity (f – fluid, w – wall, o – rod);

ϕ = angular position;

t_f, t_w = fluid temperature, wall temperature;

($\bar{t}_w$ = wall temperature, averaged over the perimeter);

q = heat flux through unit area at the heat transfer surface;

α = heat transfer coefficient;

ζ = friction factor defined by $\frac{dp}{dz} = \zeta \frac{\gamma}{d_r} \frac{u_m^2}{2g}$

Dimensionless Groups

$$T^* = \frac{q}{\rho c_p \sqrt{\frac{\tau}{\rho}}};\quad T^+ = \frac{t}{T^*};\quad y^+ = \frac{y\sqrt{\tau/\rho}}{\nu};\quad y^{++} = y^+ Pr;\quad T_f = \frac{t_w - \bar{t}_w}{\bar{q} R_2} \lambda_f$$

The rest of nomenclature is well-known.

LIST OF REFERENCES

1. *P.L.Kirillov*, "*Atomnaya energia*", *13*, *No.*5, (1962), 481.
2. *V.I.Subbotin, M.K.Ibragimov, M.N.Ivanovsky, M.N.Arnoldov, E.V.Nomofilov*, "Atomnaya energia", 10, No.4 (1961), 384 and II, No.2, (1961), 133.
3. *V.I.Subbotin, M.K.Ibragimov, E.V.Nomofilov*, "Atomnaya energia", 13, No.2, (1962), 155 and 14, (1963), 414; "Teploenergetika", No.6, (1963), 70.
4. *V.I.Subbotin, P.A.Ushakov, A.V.Zhukov, B.N.Gabrianovitch, V.D.Talanov, I.P.Sviridenko*, "Atomnaya energia", 9, No.6, (1960), 461 and 13, No.2, (1962), 162.
5. *J.Weisman* "Nuclear Science and Engineering", 6, No.1, (1959), 78.
6. *V.I.Subbotin, P.A.Ushakov, A.N.Zhukov*, "Inzhenerno-fizicheski zhurnal", 4, No.3, (1961), 3.
7. *A.Ya.Inayatov, M.A.Mikheev*, "Teploenergetika", No.3, (1957), 48.
8. *V.M.Borishanski, E.V.Firsova*, "Zhidkie metally", Gospolitizdat, M., 1963, 165.
9. *V.I.Subbotin, P.A.Ushakov, B.N.Gabrianovitch*, "Atomnaya energia", 9, No.4, (1960), 308.
10. *D.J.Gunn, G.W.Darling*, "Trans. Inst. Chem. Energ." v. 41, (1963), 163.
11. *R.I.Hodge*, Trans. ASME", ser.c, v.83, (1961), 384.
12. *R.Lyon, A.Fost, A.Katz*, "Chem. Eng. Progress", symposium series, v.51, No.7, (1955), 41.
13. *R.C.Noyes*, "Trans. ASME", series c, No.2, (1963), 125.
14. *N.Madsen, C.Bonilla*, "Chem. Eng. Progress", Symposium series, v.56, No.30, (1960), 251.
15. *P.Ya.Kucherov, L.E.Rikenglaz*, "Doklady AN SSSR, 133, No.5, (1960), 1130.

32ε

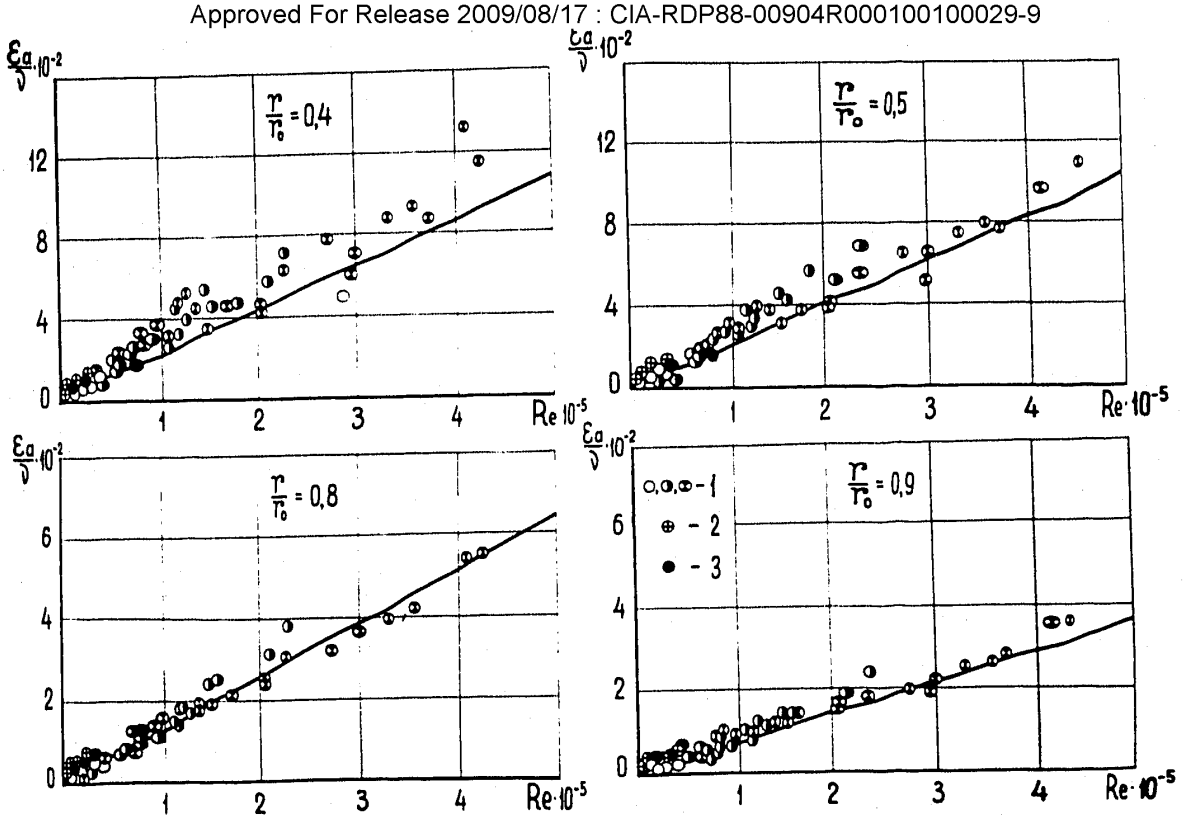

FIG.1. EDDY DIFFUSITIVITIES VERSUS Re: 1 – LIQUID METALS; 2, 3 – WATER AND AIR, RESPECTIVELY

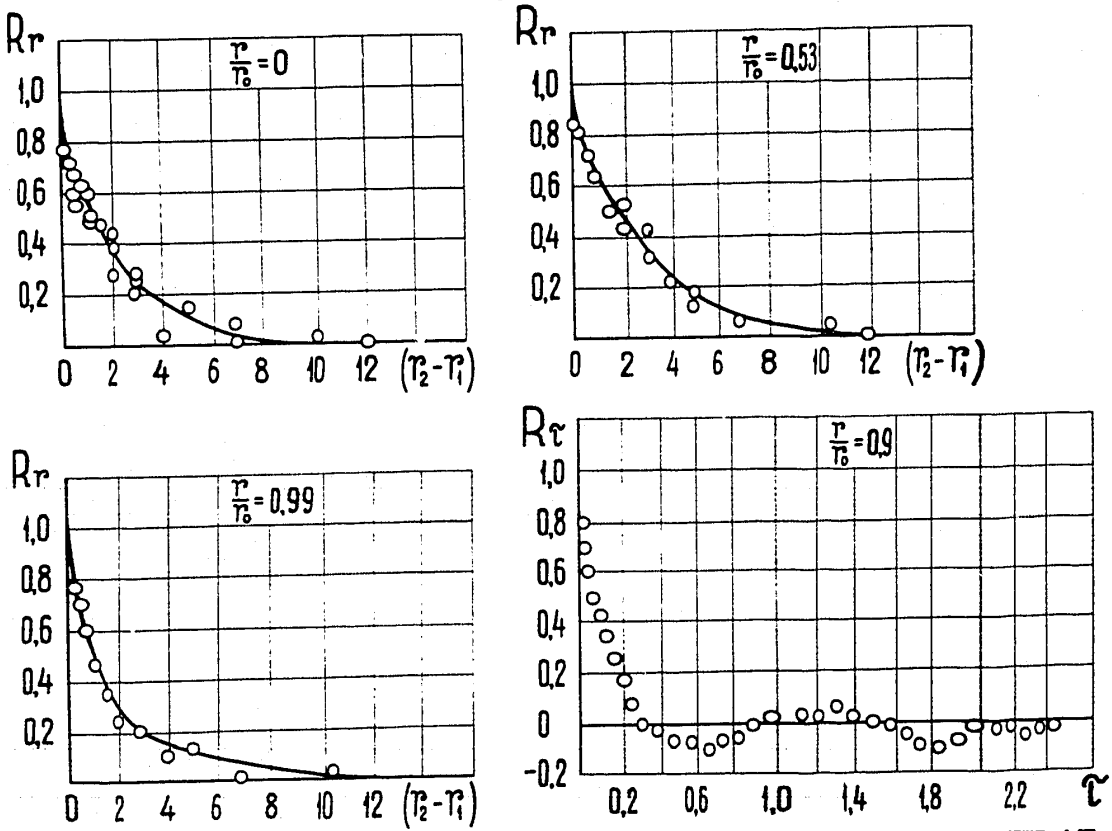

FIG.2. CORRELATION COEFFICIENTS: R_τ – FROM THE EXPERIMENTS WITH WATER AT $Re = 17 \times 10^3$; AND R_τ – FROM THE EXPERIMENTS WITH MERCURY AT $Re = 10^5$

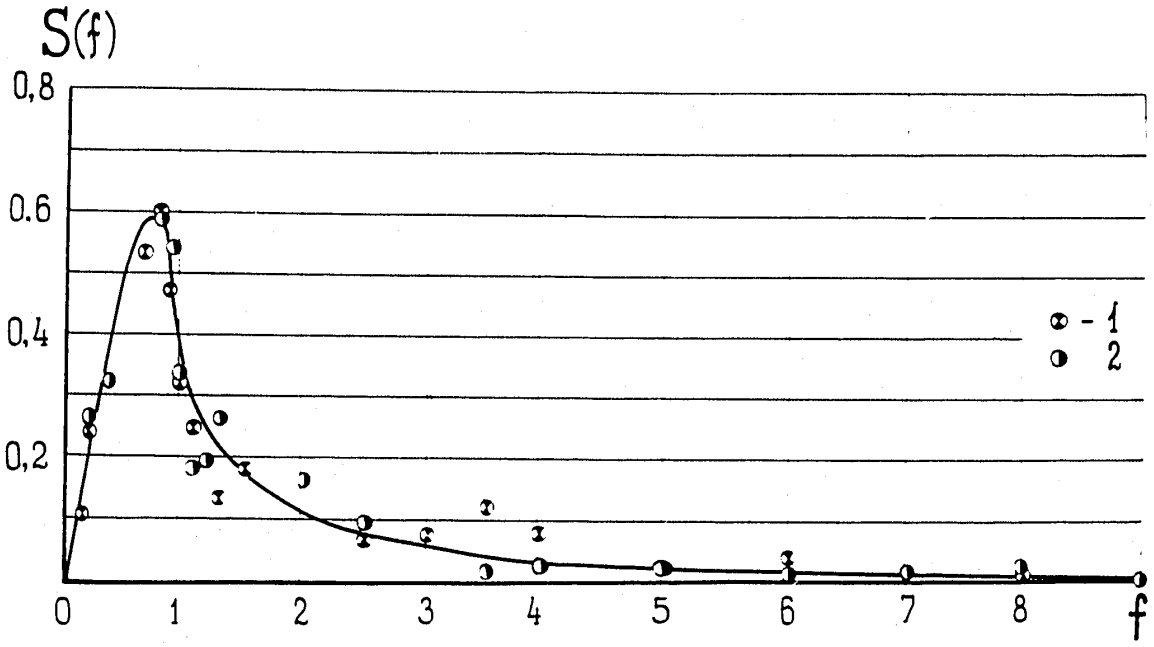

FIG.3. DENSITY OF SPECTRAL FUNCTION S(f) FROM THE EXPERIMENTS WITH MERCURY 1.2 – AT $\frac{r}{r_o}$ = 0 AND 0.9, RESPECTIVELY

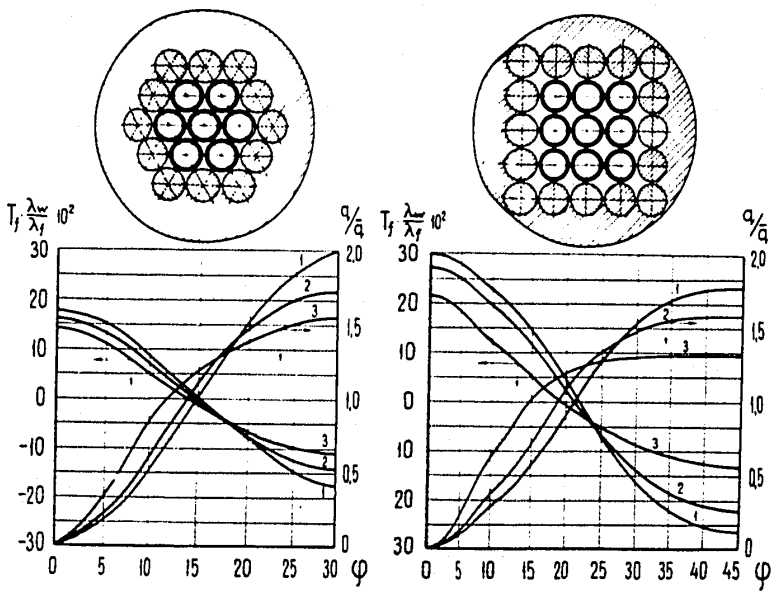

FIG.4. CIRCUMFERENTIAL TEMPERATURE AND HEAT FLUX DISTRIBUTION IN CLOSE-PACKED ROD BUNDLES WITH TRIANGULAR AND SQUARE ARRAYS. 1, 2, 3 – MERCURY ($\frac{\lambda_w}{\lambda_f}$ = 1.85), Na-K ALLOY ($\frac{\lambda_w}{\lambda_f}$ = 0.69) AND WATER ($\frac{\lambda_w}{\lambda_f}$ = 24), RESPECTIVELY

326

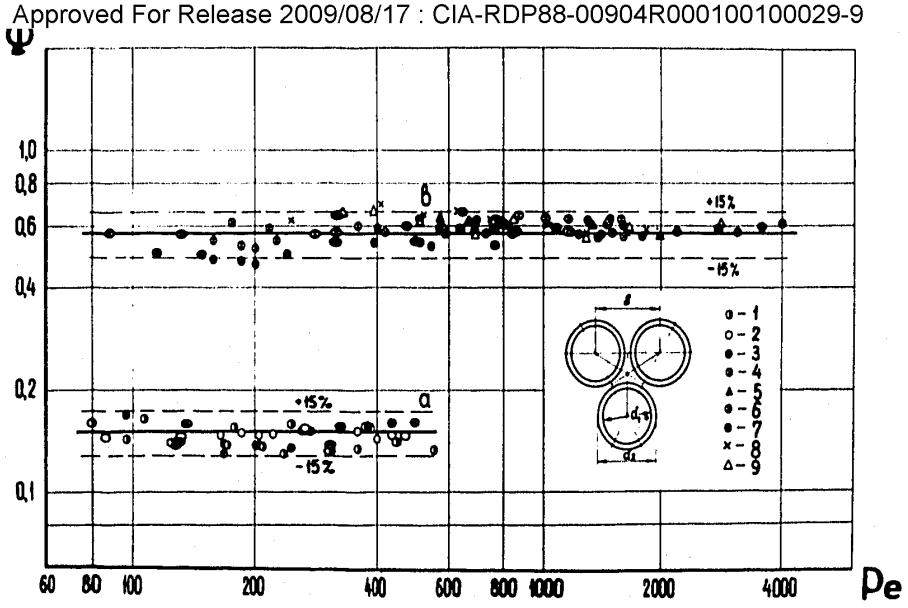

FIG.5. HEAT TRANSFER TO LIQUID METALS IN ROD BUNDLES. CLOSE-PACKED BUNDLES (a): 1, 2, 3 – $\frac{\lambda_w}{\lambda_f}$ = 0.69, 1.85 AND 16.3, RESPECTIVELY. LOOSE-PACKED BUNDLES (b): 4, 5, 6, 7, 8, 9 – s/d_2 = 1.1; 1.15; 1.2; 1.3; 1.4; 1.5, RESPECTIVELY

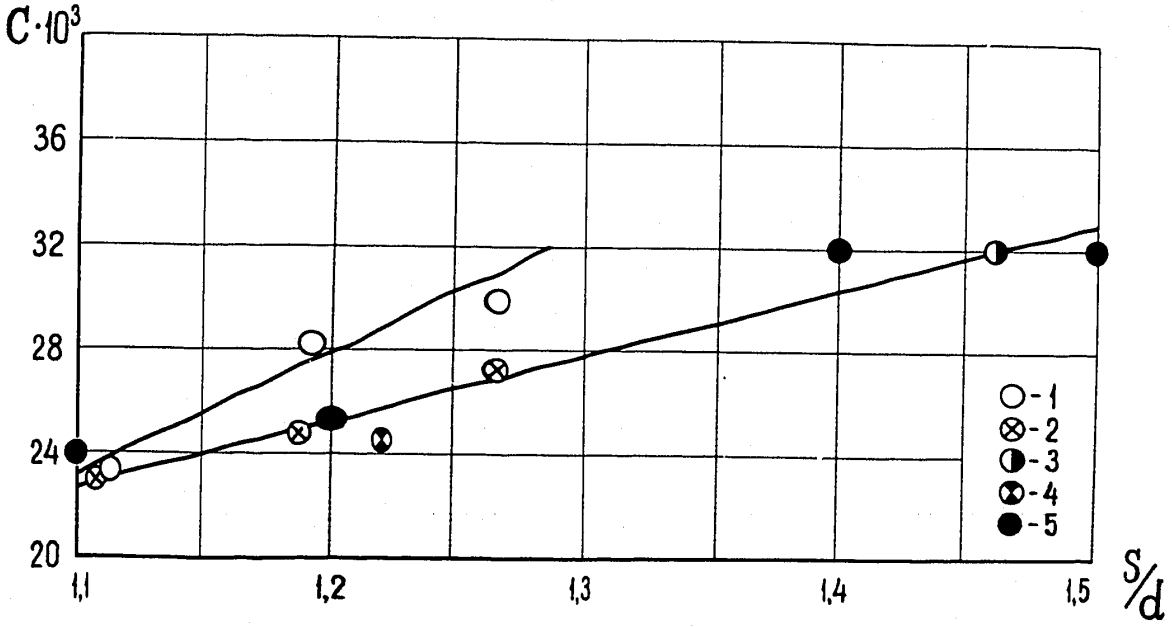

FIG.6. COMPARISON OF DATA FOR WATER WITH FORMULA (21).1, 2, 3 – DATA OF DINGEE ET AL. FOR SQUARE AND TRIANGULAR ARRAYS (TAKEN FROM [5]; 4 – DATA OF PAPER [7]; 5 – FROM THE EXPERIMENTS CARRIED OUT BY B.N.GABRIANOVITCH, A.V.ZHUKOV, P.A.TITOV, P.A.USHAKOV

328

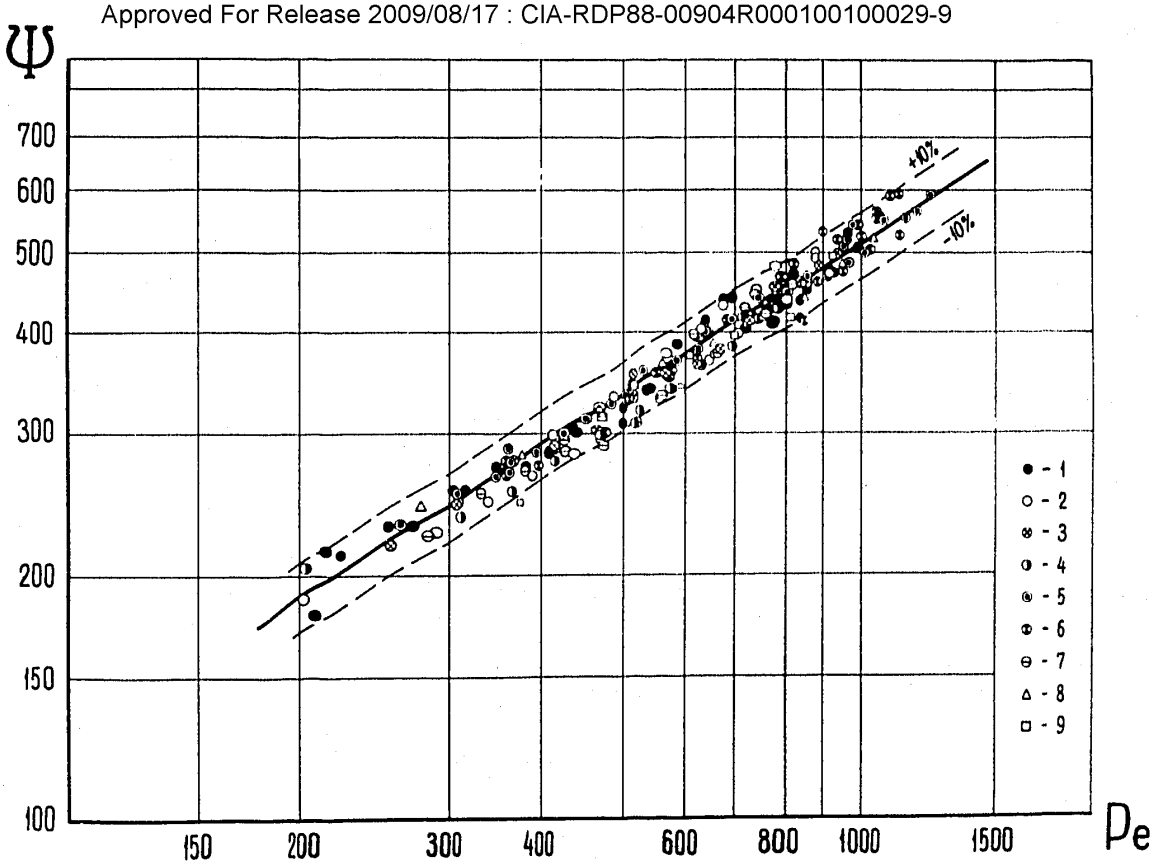

FIG.7. MEAN VALUES OF SHELL SIDE NUSSELT NUMBER Nu FOR 1 – s/d_2 = 1.1, l = 425 mm; 2, 3, 4 – s/d_2 = 1.14, l = 314, 500 AND 600 mm; 5, 6, 7 – s/d_2 = 1.25, l = 514, 765 AND 1040 mm; 8, 9 – s/d_2 = 1.4, l = 460 AND 1300 mm, RESPECTIVELY

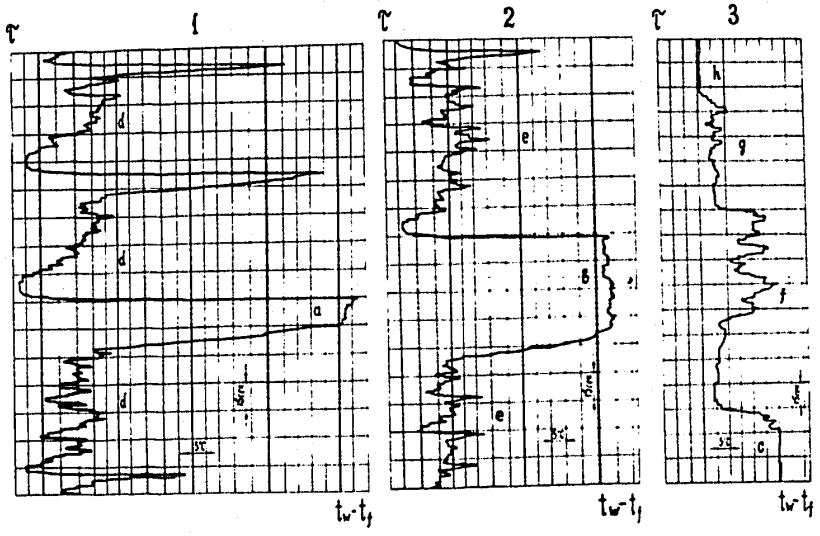

FIG.8. WALL TEMPERATURE VERSUS TIME FOR SODIUM BOILING 1, 2, 3 – q = = $1.4 \cdot 10^6$; $0.82 \cdot 10^6$; $0.47 \cdot 10^6$ $\frac{kcal}{m^2 h}$ AND t_s = 710, 690, 800°C, RESPECTIVELY

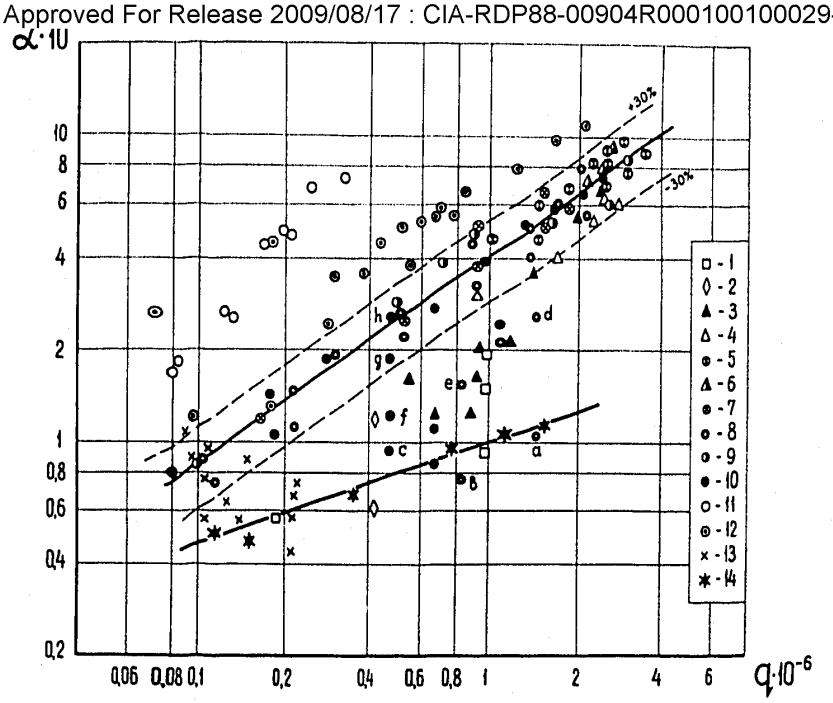

FIG.9. HEAT TRANSFER TO BOILING SODIUM UNDER FREE CONVECTION CONDITIONS 1, 2, 3 – NICKEL SURFACE, t_s = 600, 650 AND 700°C; 4, 5, 6, 7–COPPER SURFACE, t_s = 700, 750, 800 AND 850° C; 8, 9, 10 – STAINLESS STEEL SURFACE, t_s = 700, 800 AND 850°, RESPECTIVELY; 11, 12 – DATA FOR SODIUM FROM [12, 13]; 13 – DATA FOR NaK FROM [14]; 14 – FREE CONVECTION WITHOUT BOILING (t_f = 500°C, p = 1 atm)

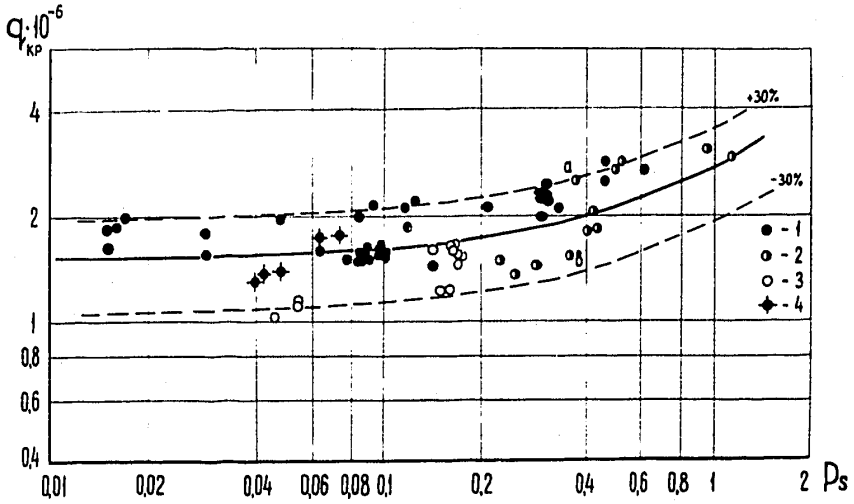

FIG.10. BURNOUT HEAT FLUXES IN SODIUM BOILING UNDER FREE CONVECTION CONDITIONS 1,2,3 – ON NICKEL-BASE HIGH-TEMPERATURE ALLOY, ON MOLYBDENUM AND ON STAINLESS STEEL, RESPECTIVELY; 4 – DATA OF PAPER [13]

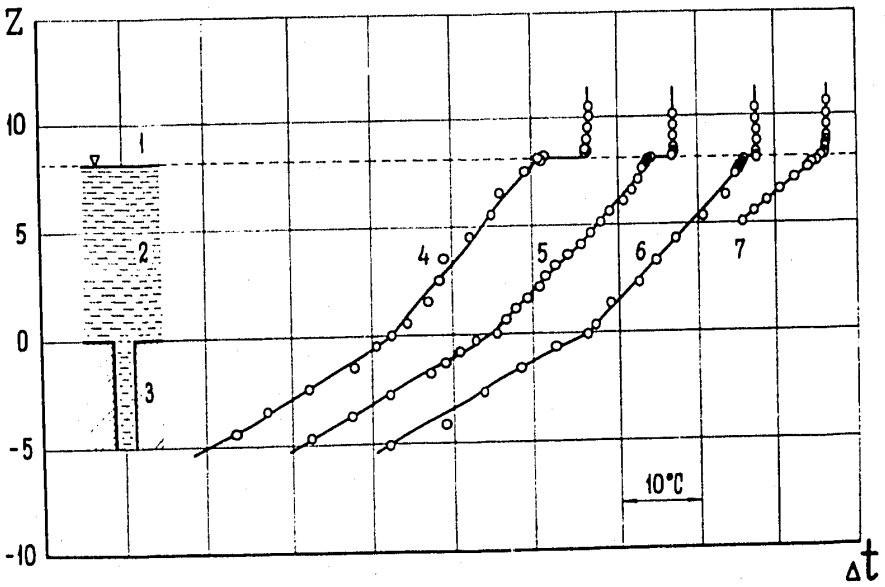

FIG.11. TEMPERATURE DISTRIBUTION IN POTASSIUM VAPOUR, CONDENSATE AND CONDENSER WALL 1, 2, 3 – VAPOUR, CONDENSATE AND WALL; 4, 5, 6, 7 – DATA AT VAPOUR TEMPERATURES 345, 364, 383 AND 640°C, RESPECTIVELY

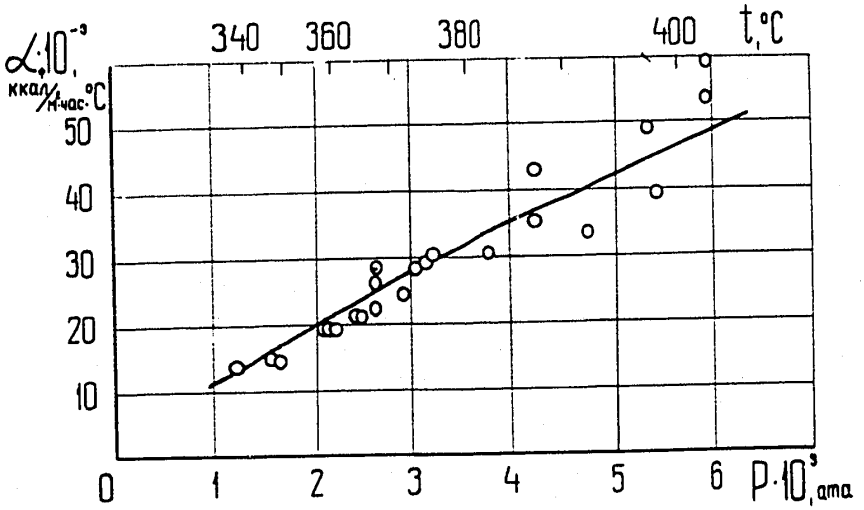

FIG.12. COMPARISON OF POTASSIUM CONDENSATION COEFFICIENTS CALCULATED FROM THE TEMPERATURE "JUMP" AT THE VAPOUR-LIQUID INTERFACE AND PREDICTED BY KINETIC THEORY OF GASES

328